Geochimica et Cosmochimica Acta, Vol. 69, No. 17, pp. 4237–4252, 2005

0016-7037/05 $30.00 + .00

doi:10.1016/j.gca.2005.04.005

# Effects of intracellular structural associations on degradation of algal chloropigments in natural oxic and anoxic seawaters

HAIBING DING and MING-YI SUN*
Department of Marine Sciences, University of Georgia, Athens, GA, 30602, USA

(*Received August* 25, 2004; *accepted in revised form April* 12, 2005)

**Abstract**—To understand the effects of intracellular structural associations on degradation of algal chloropigments, we conducted a series of microcosm experiments by incubating *Emiliania huxleyi* cells (a marine haptophyte) in natural oxic and anoxic seawaters collected from a stratified water column in the Cariaco Basin. The incubated cell detritus were sequentially treated with two buffer solutions to separate pigment components into soluble and insoluble fractions. By using non-denaturing gel electrophoresis, several chlorophyll-complexes, free chlorophyll, and another unknown chlorophyll-containing component were further separated from the soluble fraction. The chlorophyll-complexes included those bound with high molecular weight core-proteins (CP-I and CP43+CP47) and low molecular weight polypeptides (LHC-I and LHC-II) in the cellular photosystems PS-I and PS-II. Overall pigment recovery from these fractions and gel bands was well equivalent to the total amount from direct acetone extraction of the cells. We followed the time-dependent concentration changes of chlorophyll-a (Chl-a), phaeophorbide-a (Ppb-a), and phaeophytin-a (Ppt-a) in all fractions and complexes to estimate the degradation rate constants of chloropigments in natural oxic and anoxic seawaters. Our experimental results demonstrated that the intracellular structural associations had important influences on degradation of chloropigments under different redox conditions. In general, total Chl-a degraded faster (~4X) in oxic seawater than in anoxic seawater. However, the rate differences between oxic and anoxic conditions varied among the fractions and complexes. Degradation rate constants of Chl-a in soluble fraction were much higher (>10X) than those in insoluble fraction under both oxic and anoxic conditions. Chl-a bound with the complexes in PS-II appeared to be more reactive (~2X) than that in PS-I under oxic conditions but the difference in degradation rate constants between two photosystems became indistinguishable under anoxic conditions. Variations of Ppb-a in different fractions and complexes during incubation showed different patterns, implying that cellular Chl-a could degrade through two different pathways: (1) internal degradation into Ppb-a within insoluble pool and polypeptide complexes; and (2) release first from protein complexes and followed by external degradation. 

## 1. INTRODUCTION

Carbon cycling is one of the most important factors affecting global climate change (Berger and Keir, 1984; Ikeda and Tajika, 2003). Phytoplankton production and its degradation in marine systems consist of a biologic pump, driving carbon cycling in water column and sediments (Keely and Brereton, 1985; Pedersen and Calvert, 1990; Harvey et al., 1995). Studies of carbon cycling have been greatly advanced by refined knowledge on the variations of individual organic compounds (biomarkers) in marine systems (Wakeham and Beier, 1991; Sun et al., 1991; Squier et al., 2002). For example, chlorophyll-a (Chl-a), a major pigment in almost all phytoplankton species, is commonly used as biomass index while its primary derivatives (phaeopigments), which are produced during various biochemical processes, have been often used as indicators to examine organic matter degradation (Welschmeyer and Lorenzen, 1985; Carpenter et al., 1986; Furlong and Carpenter, 1988; King and Repeta, 1994). More Chl-a degradation products were also found in recent sediments due to diagenetic processes (Schaeffer et al., 1993; Ocampo and Repeta, 1999; Ocampo et al., 1999). However, the degradation mechanisms of Chl-a, especially in variable environments, have not been completely understood (Hendry et al., 1987; Keely and Maxwell, 1991; Chen et al., 2003).

Previous studies have shown that natural cell-associated Chl-a degraded differently under variable redox conditions (Sun et al., 1993a, 1993b; Bianchi et al., 2000). The Chl-a degraded faster and more completely under oxic conditions than under anoxic conditions. There was always a significant proportion of Chl-a remaining stable under anoxic conditions. However, when free Chl-a tracers were incubated in oxic and anoxic sediments, the difference between oxic and anoxic degradation processes became insignificant (Sun et al., 1993a). It is unclear why the cell-associated Chl-a has different behavior from free Chl-a during degradation. However, it was suspected that the structural associations of Chl-a with other compounds within the cells might exert critical influences on Chl-a degradation (Schoch and Brown, 1987; Louda et al., 1998).

Within the algal cells, Chl-a and other pigments are non-covalently bound to various proteins and polypeptides to form several complexes and the assembly of these complexes builds up two photosystems (PS-I and PS-II), which are embedded in the thylakoid membrane and drive photosynthesis (Golbeck, 1992; Barber, 1998, 2002; Fromme et al., 2001; Tetenkin, 2003). Both PS-I and PS-II photosystems are composed of core protein complexes (CP) and light-harvesting polypeptide complexes (LHC) (Green and Durnford, 1996; Scheller et al., 2001; Bumba and Vácha, 2003; Jensen et al., 2003). Although the

* Author to whom correspondence should be addressed (mysun@uga.edu).

sizes, structures, and functions of various chlorophyll-protein and chlorophyll-polypeptide complexes are generally known (Barber et al., 2000; Ben-Shem et al., 2003; Liu et al., 2004), few studies have been conducted to examine how these complexes affect Chl-a degradation in natural oxic and anoxic environments.

Several methods have been developed to extract and separate chlorophyll-protein complexes (Picuad et al., 1982; Schoch and Brown, 1987; Kashino, 2003). Principally, four major steps are required to characterize chlorophyll-protein complexes from algal and plant cells: (1) breaking of cell wall by homogenization; (2) solubilization of the complexes from cell membrane with buffer solutions containing detergents; (3) separation and identification of complexes by gel electrophoresis; and (4) qualitative and quantitative analyses of pigments from the separated complexes after further extraction (Zolla et al., 1997; Almela et al., 2000). Although these methods have been successfully used to extract, separate, purify, identify and quantify the chlorophyll-protein complex compositions in various algal and plant cells, there is an uncertainty on the recovery of Chl-a from various complexes. It is also unclear whether there are other potential structural components, in addition to chlorophyll-protein and chlorophyll-polypeptide complexes, that bind Chl-a within the cells.

This study was designed to examine the effects of intracellular structural associations of chloropigments with other molecular matrixes on Chl-a degradation in natural oxic and anoxic seawaters. Our specific goals are: (1) to differentiate structural pools containing Chl-a, including various complexes; (2) to test the recovery of Chl-a from various pools during extraction and separation processes; (3) to determine degradation rates of Chl-a in various pools under oxic and anoxic conditions; and (4) to examine the possible degradation pathways of Chl-a in different pools. We conducted a series of experiments by incubating *E. huxleyi* cells in natural oxic and anoxic seawaters collected from a stratified water column in the Cariaco Basin. We monitored the variations of bacterial abundances and three bacteria-specific fatty acids in two systems to understand the bacteria community. We followed the time-dependent variations of Chl-a, phaeophorbide-a (Ppb-a), and phaeophytin-a (Ppt-a) in total pigment pool and in different structural pools. Degradation rate constants of Chl-a in different pools were estimated by fitting data with a multi-G model (Berner, 1980) while the variations of Ppb-a in different pools were quantitatively described with a release-degradation model (Sun et al., 1993b). In addition, the degradation pathways of Chl-a in various pools were examined based on the relative variations of Chl-a and phaeopigments.

## 2. EXPERIMENTAL

### 2.1. Materials and Microcosm Setup

The natural oxic and anoxic seawaters used in our experiments were collected in May 2001 from a stratified water column in the western Cariaco Basin (10°30′N, 64°40′W) during cruise 66 of the CARIACO time series on the R/V Hermano Ginés. At this time, the oxic/anoxic boundary in the water column was at ~350 m depth. Oxic seawater was collected from 30 m and anoxic seawater from 930 m using a set of 12-L Teflon-coated Niskin bottles. A nitrogen line was fitted to the upper vent of the Niskin bottles for collecting anoxic seawater. Seawater samples were unfiltered and directly transferred to prerinsed 2-L plastic screw-topped bottles. For anoxic seawater samples, the bottles were placed in sealed plastic bags filled with nitrogen. The laboratory incubation experiments were set up 10 days after the water samples were collected.

The marine haptophyte *E. huxleyi* (clone CCMP 1949) was obtained from the Provasoli-Guillard National Center for culture of marine phytoplankton, Booth Bay Harbor, Maine, USA. This alga was first cultured in 50 mL f/50 medium at 14°C and then transferred to 250 mL medium in 10 days (before the end of exponential growth phase). After another 10 days, the culture was separated into four flasks with 1000 mL medium in each. The algal cells in the final medium were harvested by centrifugation after 10 days and stored at −20°C for later incubation experiments. The culturing was carried out in a 12:12 light/dark regime.

The incubation microcosm consisted of a series of 500 mL flasks filled with 200 mL oxic or anoxic seawater. ~450 mg thawed (~90% water) algal cells were added into each flask, resulting in a ~20 mg/L organic carbon load in the microcosms. Setup of anoxic incubations, including transfer of seawater and addition of cell materials, was conducted in a $N_2$-filled plastic bag. Oxic incubations were set up in open air. All flasks were sealed with stoppers (a switch being inserted for gas purging) and the flasks with anoxic seawater were flushed with $N_2$ for one minute before sealing. Oxic incubations were conducted in an open air chamber while anoxic incubations in a $N_2$-filled chamber. Two chambers were kept in an incubator at 15°C and in the dark. During incubation, water-saturated air and $N_2$ were separately purged into the oxic and anoxic seawater samples frequently (several times per day) to maintain the original redox conditions. At $t = 0$, two flasks (duplicate) were immediately used for sample treatment as an initial point and at 5, 10, 17, 24, 35, 50, 70 and 90 days, one oxic and one anoxic flask were taken out from each chamber. A subsample (100 mL) from each flask was used for extraction, separation, and analysis of pigment complexes while another subsample (50 mL) was used for lipid analysis. In addition, a small volume (10 mL) of sample was used for total pigment analysis by direct acetone extraction while another 1 mL was used for counting bacterial abundance. All detritus in the incubated samples was collected by centrifugation and stored frozen (−40°C) for later extraction and analysis.

### 2.2. Analysis of Bacteria-Specific Fatty acids and Bacteria Counting

Details for extraction and analysis of lipids in these incubated samples were reported elsewhere (Sun et al., 2004). Briefly, the detritus centrifuged from 50 mL incubated subsample was first extracted with 10 mL methanol, followed by 3 × 10 mL methylene chloride-methanol (2:1 v/v) extraction. Combined extracts were saponified with 0.5 M KOH in MeOH/$H_2O$ (95:5) to separate neutral and acidic lipids. Neutral lipids were first extracted from the basic solution (pH >13) with hexane while fatty acids were then extracted with hexane after addition of HCl into the solution (pH <2). Fatty acids in the acidic extracts were methylated with 5% $BF_3$-methanol to form

fatty acid methyl esters (FAMEs). FAMEs were analyzed by capillary gas chromatography (GC) using a Hewlett-Packard 6890 GC system with an on-column injector and a flame ionization detector. Compound separation was achieved by a 30 m × 0.25 mm i.d. column coated with 5%-diphenyl-95%-dimethylsiloxane copolymer (HP-5, Hewlett-Packard). Selected samples were analyzed by gas chromatography-mass spectrometry (GC-MS) to identify bacteria-specific fatty acids. GC-MS analysis was performed on a SHIMADZU QP5000 GC-MS system using a 30 m × 0.25 mm i.d. column coated with 5% phenyl methyl silicone (XTI-5, Restek).

Bacterial counting was performed based on published methods (Porter et al., 1980; Suzuki et al., 1993). First, 1 mL incubated seawater sample containing detritus was mixed with 1 mL 4′,6-diamidino-2-phenylindole solution (DAPI, 33 μg/ml) and then passed through 0.2 μm black filter. After filtration, the black filter was mounted on a slide and the bacterial numbers on the filter was counted with an oil-immersion lens under a microscope. Bacterial abundance was estimated by averaging 10 countings.

### 2.3. Extraction and Separation of Pigments in Different Structural Pools

Total pigment concentrations (T) were determined by direct extraction of detritus, which was centrifuged from 10 mL incubated seawater, with 2 × 5 mL acetone. The extraction and separation of pigments in different structural components were carried out generally based on a modified version of the method of Picaud et al. (1982). The detritus (centrifuged from 100 mL incubated seawater) were first treated in a 5 mL buffer-1 solution (2 mM trismaleate, 0.1 M sorbitol, 0.5 mM amino caproic acid and 1 mM phenylmethylsulfonyl fluoride) with a homogenizer for 2 min. After centrifugation at 4500 rpm at 4°C for 10 min, the supernatant was removed and acetone was added to the solution with a final volume of 20 mL as fraction 1 (F1). The detritus were then treated in a 2 mL buffer-2 solution (2 mM trismaleate and 20 mg/ml digitonin) with an ultrasonicator for 20 s and followed by 1 h vortex. Solubilized pigment components were separated from the detritus by centrifugation at 5500 rpm (4°C) for 20 min. The extracted detritus were treated again in the same way. The combined supernatant, which contained solubilized pigment components, was defined as a soluble fraction (F2). Usually, 1 mL of F2 extract was diluted with acetone to 10 mL for direct pigment analysis while rest of the F2 extract was used for further separation of soluble pigment components by electrophoresis. The final residues were further extracted with 20 mL acetone and centrifuged at 5500 rpm for 10 min. The acetone extract from the final residue was defined as insoluble fraction (F3). All operations were conducted under subdued light to avoid potential photodegradation.

### 2.4. Separation and Identification of Soluble Pigment Components

The soluble pigment components in F2 fraction were separated by polyacrylamide gel electrophoresis (PAGE) (Picaud et al., 1982; Itagaki et al., 1986). The gel plate consisted of a stacking part and a separation part. The stacking gel was composed of 4% (w/v) acrylamide and 0.1% (w/v) N,N′-methylene-bisacrylamide, buffered by 0.375 M trisHCl (pH = 6.8). The separating gel contained 4.5% (w/v) acrylamide, 0.23% (w/v) N,N′-methylene-bisacrylamide, and 0.5% (w/v) deoxycholic acid sodium salt, buffered by 0.125 M trisHCl (pH = 8.8). Ammonium persulfate (0.05%) and 0.005% N,N,N′,N′-Tetramethylethylenediamine (TEMED) were used to polymerize both stacking and separating gels. The length ratio of stacking to separation gel was ~1:2.5.

To identify soluble pigment components, PAGE was first run on a small plate (10 × 10 cm, and 0.75 mm of thickness). Before PAGE separation, the fraction F2 was mixed with buffer-3 (60% glycerol in 0.5 M trisHCl, pH = 6.8) (2:1, v/v). The mixture (40 μL) was loaded onto the top of gel plate and a BenchMark standard (15 recombinant proteins with molecular weight ranging from 10 to 220 kDa, Invitrogen) was parallelly loaded on the same gel plate as compound markers. For comparison purpose, the extract from spinach leaves using the same procedure was also loaded on the same gel plate side by side with algal extract. Electrophoresis was carried out at 4°C and in dark with a 2 mA current for 40 min and then with a 4 mA current for 2 hours. The gel running buffer was made of 0.3% trisbase, 1.44% glycine and 0.05% sodium deoxycholate. To make the separated components visible, a Commassie Brilliant Blue dye (*R*-250) was used to stain the proteins and peptides in the gel.

To determine the pigment concentrations in various structural pools from the incubated samples, 1 mL mixture of F2 with buffer-3 (2:1, v/v) was loaded onto a large gel plate (15 × 25 cm, and 0.75 mm of thickness). Electrophoresis was conducted at a 2 mA current for 3 hrs and then a 4 mA current for 7 hrs. After the separation was achieved, all green and green-yellow bands were separately cut off from the gel and ground in 1 mL water by homogenizer. Then, acetone was added to extract pigments twice (2 × 5 mL). Each extract was centrifuged to separate pigments from the ground gel and then combined for HPLC analysis. The extraction and separation of pigment components, including total pigment (direct acetone-extracted) and various structural pools were schematically summarized in Figure 1.

### 2.5. Pigment Analysis

Pigment concentrations in the extracts from all fractions and separated bands were determined by ion-pairing reverse-phase high-performance liquid chromatography (Mantoura and Llewellyn, 1983). The HPLC system consisted of a Hewlett Packard 1100 series with a quaternary pump and a variable wavelength detector. Column used was a 5 μm C-18 (ODS) Alltech column (250 × 4.6 mm i.d.) and detection was accomplished by measuring absorbance at a wavelength of 440 nm. After injection of 100 μL extract sample, a gradient program ramped from 100% eluant A (80% methanol and 20% aqueous solution of 0.5 mM tetrabutyl ammonium acetate and 10 mM ammonium acetate) to 100% eluant B (20% acetone in methanol) in 10 min with a hold for 30 min. Authentic Chl-a standard was obtained from Sigma Chemical Co. The Ppt-a standard was prepared by acidification of Chl-a standard. The Ppb-a standard was made from *Skeletonema costatum* cells according to the procedure used by Barrett and Jeffrey (1971).

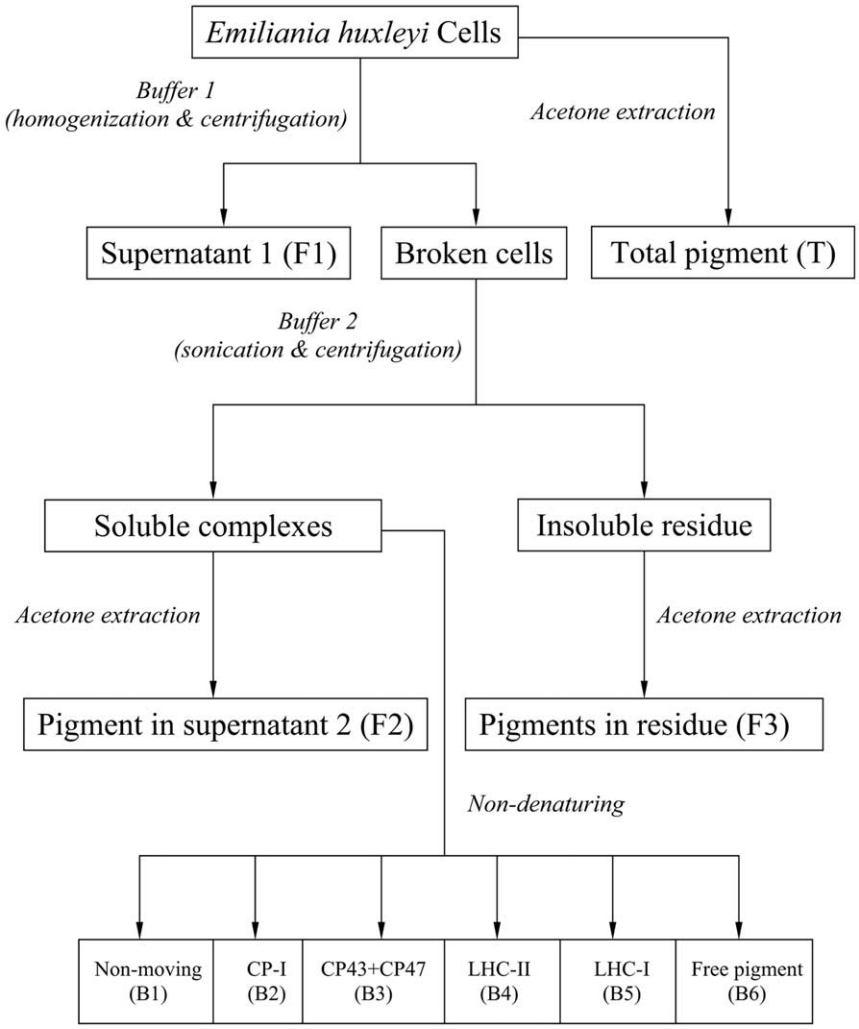


Fig. 1. An overview of extraction and separation schemes for intracellular pigment complexes from *E. huxleyi* cells.

All standards were quantified spectrophotometrically (Shimadzu UV-2501 PC spectrophotometer) using published extinction coefficients (Mantoura and Llewellyn, 1983). Identification of chloropigments in the samples was confirmed by co-injecting standards and sample extracts in HPLC.

## 3. RESULTS

### 3.1. Variations of Bacteria-Specific Fatty Acids and Bacterial Abundance

Three typical bacteria-specific fatty acids (iso-15:0, antesio-15:0 and 18:1($\omega$7)) were detected in the fatty acid extracts of samples (Fig. 2a). They varied differently in oxic and anoxic systems during incubation (Fig. 3). In the oxic system, little iso-15:0 and anteiso-15:0 fatty acids were found throughout the incubation period while initial concentration of 18:1($\omega$7) fatty acid was relatively high but decreased continuously over the incubation. In the anoxic system, the concentrations of iso-15:0 and anteios-15:0 fatty acids declined continuously from the beginning of the incubation but a small amount of iso-15:0 survived after three months. By contrast, the concentration of 18:1($\omega$7) fatty acid increased slightly in the first a few days and then decreased. However, a significant proportion of 18:1($\omega$7) (40%–50% of initial concentration) remained stable after one-month under both oxic and anoxic conditions. Unlike the variations in bacteria-specific fatty acids, bacterial abundances in oxic and anoxic seawaters increased dramatically in the first week of incubation. After one week, the bacterial abundances decreased gradually to the initial levels ($\sim$2–6 $\times$ $10^8$/L). It appeared that the bacterial abundance in anoxic seawater increased to a relatively higher level than in oxic seawater.

### 3.2. Characterization of Soluble Pigment Components by PAGE

To identify soluble pigment components, we ran the protein standard (BenchMark) and the sample extracts (soluble fraction) from *E. huxleyi* cells and spinach leaves on the same PAGE plate. After separation and staining, six colored bands occurred in two sample channels and a series of proteins and polypeptides in the standard channel. One narrow green band from the samples remained at the initial loading position (in the

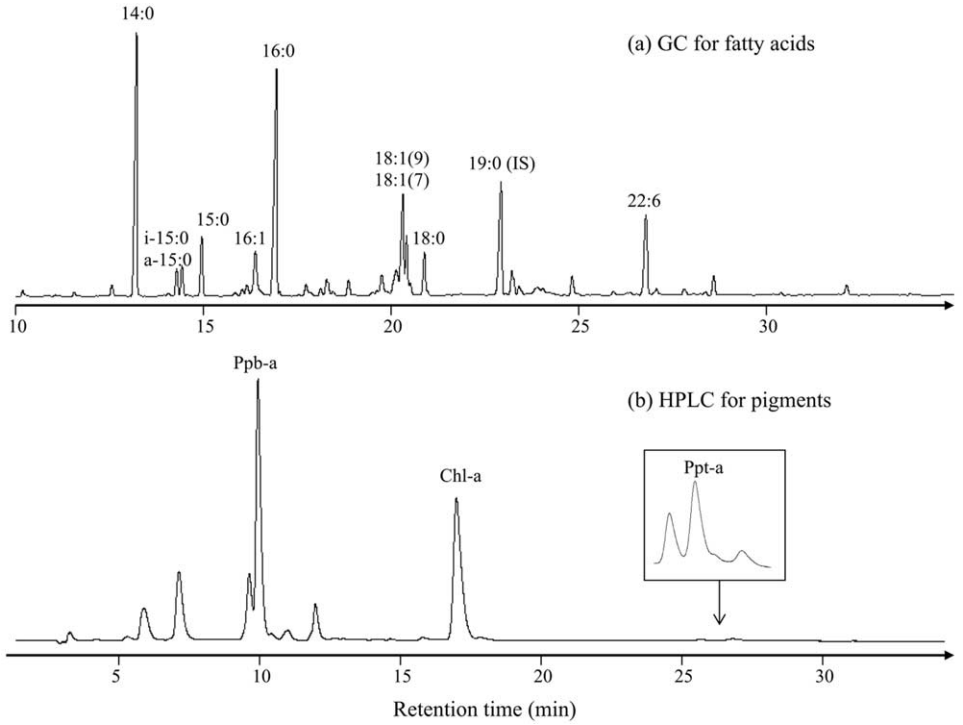


Fig. 2. (a) GC trace for identified fatty acids, where 19:0(IS) is an internal standard; (b) Reverse-phase HPLC for identified chloropigments.

stacking gel) and thus was defined as non-moving band. Other five green and green-yellow bands with variable width were well separated in the separation gel. By comparing with Bench-Mark standard, the top narrow green band in the separation gel had a molecular weight close to 160 kDa. The next wide green band had a molecular weight between 55 kDa and 60 kDa. Other two wide bands had green-yellow color and their molecular weights were relatively small (~30 kDa and ~25 kDa respectively). One narrow green band in the bottom of the gel had a molecular weight far below 10 kDa. Based on the literature (Picaud et al., 1982; Green and Durnford, 1996; Croce et al., 2002; Jackowski et al., 2003), the bands in the separation gel were characterized as CP-I (~160 kDa) and CP43+CP47 (~55–60 kDa) (core protein complexes) and LHC-II (~30 kDa) and LHC-I (~25 kDa) (antenna polypeptide complexes) in PS-I and PS-II photosystems. The bottom band is considered as free pigments due to their low molecular weights while the structural characterization of the non-moving band in the stacking gel is unknown.

### 3.3. Recovery of Chl-a from Various Fractions and Complexes

To test the recovery of Chl-a from various fractions and complexes during extraction and separation processes, we treated two identical cell samples as a duplicate measurement.

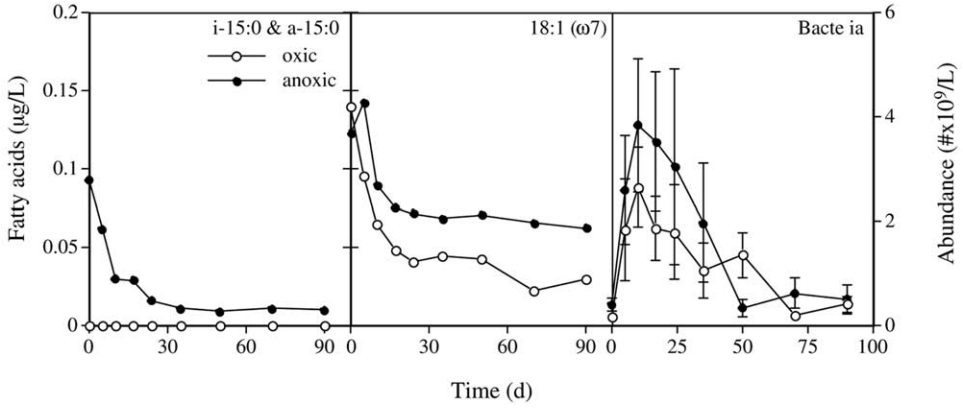


Fig. 3. Variations of bacteria-specific fatty acids (iso-15:0+anteiso-15:0, and 18:1(ω7)) and bacterial abundance during incubations in oxic and anoxic seawaters.

Table 1. Initial concentrations ($\mu$g/g wet cell material) of intracellular Chl-a bound in primary fractions* and following PAGE bands*.

| | Total Chl-a (T) | Chl-a concentration in fractions (F1) | (F2) | (F3) | Sum of fractions (F1+F2+F3) | Recovery (F1+F2+F3)/T |
|---|---|---|---|---|---|---|
| Sample-1 | 645.84 | 18 | 391.07 | 227.91 | 636.98 | 98.6% |
| Sample-2 | 617.08 | 15.6 | 378.83 | 236.45 | 630.88 | 102.2% |
| Average | 631.46 | 16.8 | 384.95 | 232.18 | 633.93 | 100.4% |
| (Error) | (±14.38) | (±1.2) | (±6.12) | (±4.27) | (±3.05) | (±1.80%) |

| | Chl-a concentration in PAGE bands (B1) | (B2) | (B3) | (B4) | (B5) | (B6) | Sum of bands (B1 to B6) | Recovery (B1 to B6)/(F2) |
|---|---|---|---|---|---|---|---|---|
| Sample-1 | 36.46 | 26.42 | 138.97 | 64.62 | 70.13 | 45.4 | 382 | 97.7% |
| Sample-2 | 33.58 | 27.06 | 129.91 | 62.44 | 72.75 | 43.42 | 369.16 | 97.5% |
| Average | 35.02 | 26.74 | 134.44 | 63.53 | 71.44 | 44.41 | 375.58 | 97.6% |
| (Error) | (±1.44) | (±0.32) | (±4.53) | (±1.09) | (±1.31) | (±0.99) | (±6.42) | (±0.1%) |

Recoveries and error ranges are estimated.
* Definitions of fractions and bands are shown in Fig. 1.

Total Chl-a concentration was determined from direct acetone extraction of the cells. The Chl-a concentrations in three fractions (F1, supernatant 1; F2, supernatant 2; and F3, residue) were determined after extracting Chl-a from these fractions with acetone. The results showed that the recovery of Chl-a from three fractions was close to 100% (Table 1). The majority of Chl-a was present in F2 (60%) and F3 (37%) fractions while only <3% of Chl-a was in F1 fraction. Thus, the small amount of Chl-a in F1 fraction was not considered in our estimation for degradation rate constants.

When the soluble pigment components in F2 fraction were further separated by the PAGE, the recovery of Chl-a from all bands reached to ~98% (Table 1) of the Chl-a in the F2. However, the distribution of Chl-a in these bands was not uniform: a maximum percentage (36%) of soluble Chl-a bound to B3 band (CP43+CP47) while a minimum percentage (~7%) in B2 band (CP-I). Two LCH complexes (B4 and B5) had 17%–19% of soluble Chl-a while ~9%–11% were in non-moving band (B1) and free pigment band (B6) respectively.

### 3.4. Variations of Total Chloropigments

In this study, three chloropigments (Chl-a, Ppb-a and Ppt-a) were identified (Fig. 2b) by co-injection with standards. Concentrations of total chloropigments (direct acetone extracted) varied differently during three-month incubation (Fig. 4). Chl-a degraded continuously in oxic and anoxic seawaters, but the initial degradation was fast in the first 10–20 days and followed by a slow degradation. There were differences in initial rate and remaining proportion between oxic and anoxic degradations of Chl-a: an apparently faster initial rate occurred in oxic seawater but a relatively larger proportion of Chl-a remained in anoxic seawater after three months. Variations of phaeopigments showed different patterns from Chl-a. In the first 10–20 days, the concentrations of Ppt-a increased slightly in both oxic and anoxic seawaters while the concentrations of Ppb-a increased apparently only in anoxic seawater. After that, the concentrations of these phaeopigments all decreased with time but relatively larger proportions remained in anoxic seawater than in oxic seawater.

### 3.5. Variations of Chloropigments in Soluble and Insoluble Fractions

Chl-a in the soluble and insoluble fractions (F2 and F3) degraded continuously with time (Fig. 5). However, Chl-a in soluble fraction appeared to degrade much faster than that in insoluble fraction. There were also apparent differences between oxic and anoxic degradations in both soluble and insoluble fractions. After three-month incubation, soluble Chl-a was almost completely degraded in oxic seawater while ~20% of initial soluble Chl-a remained in anoxic seawater. By contrast, a large proportion (>50% relative to the initial concentrations) of insoluble Chl-a remained in both oxic and anoxic seawaters after three months. Two phaeopigments (Ppb-a and Ppt-a) in the soluble and insoluble fractions followed the similar patterns to those observed in the total acetone extracted pool, but an exception (a small initial increase) was found for insoluble Ppb-a in oxic seawater (Fig. 5).

### 3.6. Variations of Chloropigments in Soluble Complex Pools

The concentrations of Chl-a in each complex pool declined continuously during incubation (Fig. 6). The Chl-a degradation in these structural components basically followed the same patterns as those observed in total acetone extracted pool and soluble fraction, that is, initial faster decrease followed by slower decrease. The differences between oxic and anoxic degradations in several pools (e.g., LHC-I and LHC-II, CP43+CP47, and the non-moving band) were still obvious while there was little difference in CP-I band. In most cases, Chl-a in the complexes degraded more completely in oxic seawater while there was always a proportion of Chl-a remaining in anoxic seawater after three months. On the other hand, variations of Ppb-a in these soluble complex pools showed different patterns (Fig. 7). For example, in the LHC-I and LHC-II pools (polypeptide complexes), concentrations of Ppb-a initially increased in the first week and then gradually decreased. By contrast, in the CP-I and CP43+CP47 pools (protein complexes), Ppb-a concentrations decreased from the

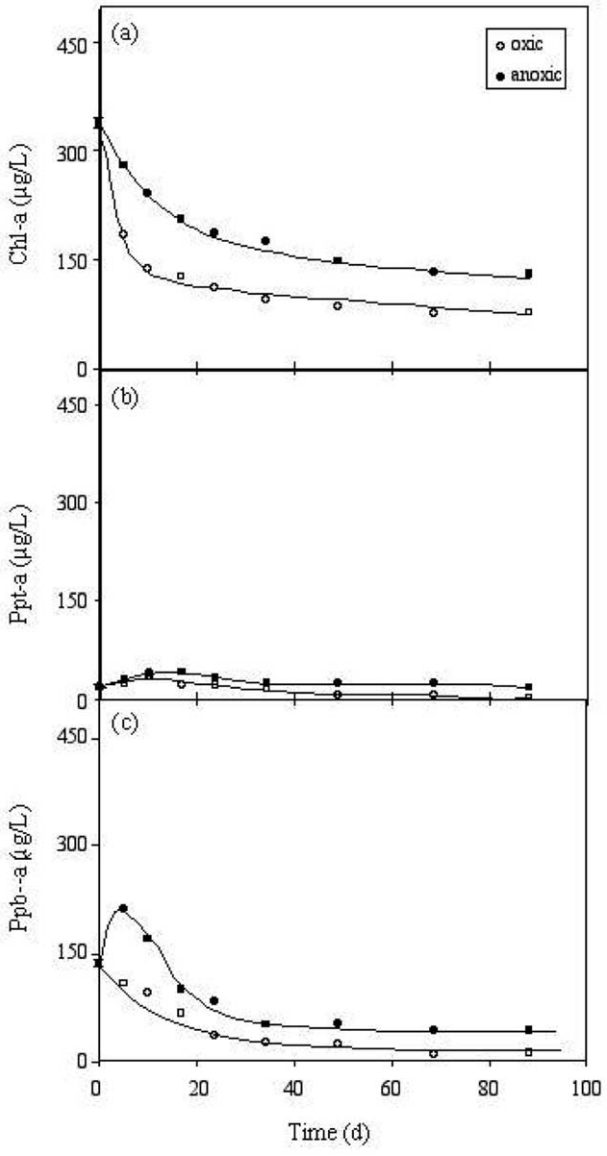


Fig. 4. Variations of total acetone-extracted Chl-a, Ppt-a and Ppb-a concentrations during incubations.

beginning of the incubation. A continuous decreasing trend of Ppb-a concentration was also observed in the non-moving band (both oxic and anoxic) and the free pigment pool although a slight increase of Ppb-a was observed in the free pool under anoxic conditions.

## 4. DISCUSSION

### 4.1. Variations of Microbial Communities in the Incubation Systems

Different bacteria communities inhabit in the stratified oxic and anoxic seawaters in the Cariaco Basin (Tuttle et al., 1977; Taylor et al., 2001). There have been intensive studies (Madrid et al., 2001; Neretin et al., 2003; Vetriani et al., 2003) demonstrating that specific microbial activities of different bacteria along the redox gradient in natural water column (e.g., the Cariaco Basin and the Black Sea) are responsible for different biochemical degradation of organic matter. The bacterial communities in oxic/anoxic water column have been characterized by several approaches, including lipid biomarkers (Wakeham et al., 1995, 2004; Saliot et al., 2002). It has been confirmed that aerobic and anaerobic bacteria have distinct fatty acid compositions (Parkes and Taylor, 1983; Keith-Roach et al., 2002). In this study, our experimental systems consisted of natural oxic and anoxic seawaters from the Cariaco water column and pure culture of *E. huxleyi* (bacteria free). The natural seawaters were unfiltered and used for the experiment in 10 days after the sampling. The initial bacterial abundances in the experimental seawaters are confirmed to be at the same level in the natural environment (Taylor et al., 2001). Our lipid analysis indeed showed the differences in bacteria-specific fatty acids between the oxic and anoxic systems (Fig. 3): little branched iso- and anteiso-15:0 fatty acids were found in the oxic system, contrasting to the anoxic system. This observation for the different fatty acid compositions between the experimental oxic and anoxic systems was consistent with the measurement for field samples (Wakeham and Ertel, 1987).

During incubation, bacterial abundances in two systems varied in a similar way: initial increase in the first week and followed by a continuous decrease but greater variation was found in the anoxic system (Fig. 3). The increase of bacterial abundance in both systems was attributed to the addition of algal materials. It was demonstrated that introduction of fresh organic matter could stimulate bacterial growth (Danovaro et al., 1994; Zweifel et al., 1996), but the bacterial abundance declined when the most bioavailable materials were consumed (Harvey et al., 1997; Puddu et al., 1998). Although the bacteria-specific fatty acids and bacterial abundance have been often used to assess bacterial biomass (Cranwell et al., 1987; Wakeham and Beier, 1991), these variations in our experimental systems were not correlated (Fig. 3). The inconsistence between bacteria-specific fatty acids and bacterial abundance (or biomass) was observed in other seawater and sediment systems (Harvey and Macko, 1997; Ding and Sun, 2005). However, the variations of the bacteria-specific fatty acids and bacterial abundance in the oxic and anoxic systems implied that different microbial processes might be involved in the degradation of cellular chloropigments.

### 4.2. Oxic vs. Anoxic Degradation of Chl-a in Various Fractions and Pools

During three-month incubation, the Chl-a concentrations in total pool, soluble and insoluble fractions, and soluble complex pools decreased rapidly in the first 10–20 days and then followed by a continuous slow decrease. This degradation pattern has been quantitatively described by a well-known multi-G model (Berner, 1980). In this model, different fractions of organic matter are assumed to have different reactivities and degrade at independent rates. The sum of each individual degradation rate equals to the overall organic matter degradation rate, as shown by the following equations:

$$-\frac{dG_t}{dt} = \sum k_i G_i \quad (1)$$

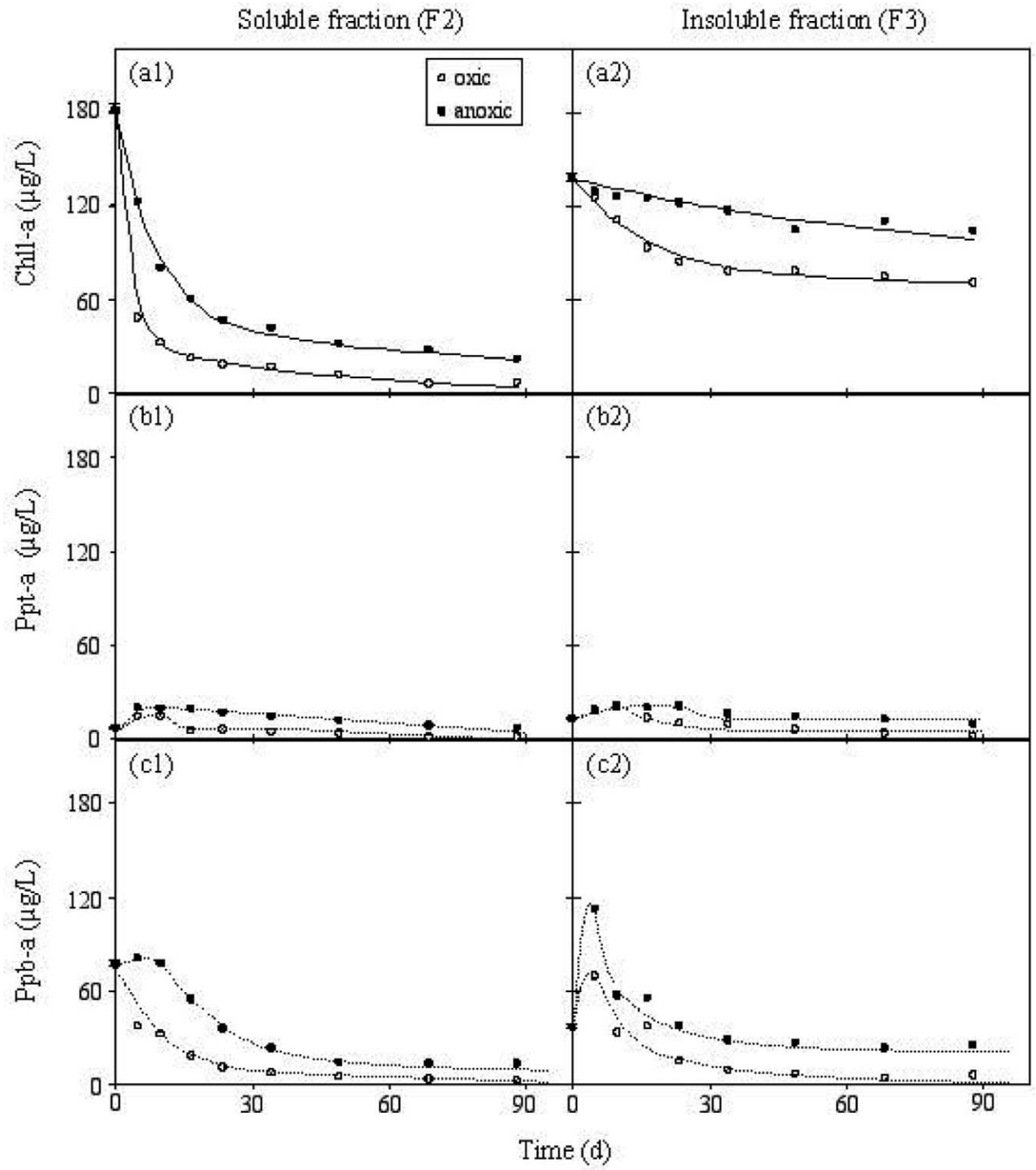


Fig. 5. Variations of Chl-a, Ppt-a and Ppb-a concentrations in soluble and insoluble fractions during incubations.

$$G_t = \sum G_i = (G_1)_0 \exp(-k_1 t) + (G_2)_0 \exp(-k_2 t) + \ldots \quad (2)$$

where $k_i$ is the first-order degradation rate constant of fraction i; $G_i$ is the concentration of fraction i and $-dG_t/dt$ is the degradation rate of all fractions; $(G_1)_o$ and $(G_2)_o$ are initial concentrations of fraction 1 and fraction 2.

The validity of multi-G model was confirmed by testing natural organic matter degradation in natural seawater and sediment systems (Westrich and Berner, 1984). This model has been extended to studies of specific organic compounds, which are bound in different fractions of organic matter (Henrichs and Doyle, 1986; Sun and Wakeham, 1998; Teece et al., 1998). In

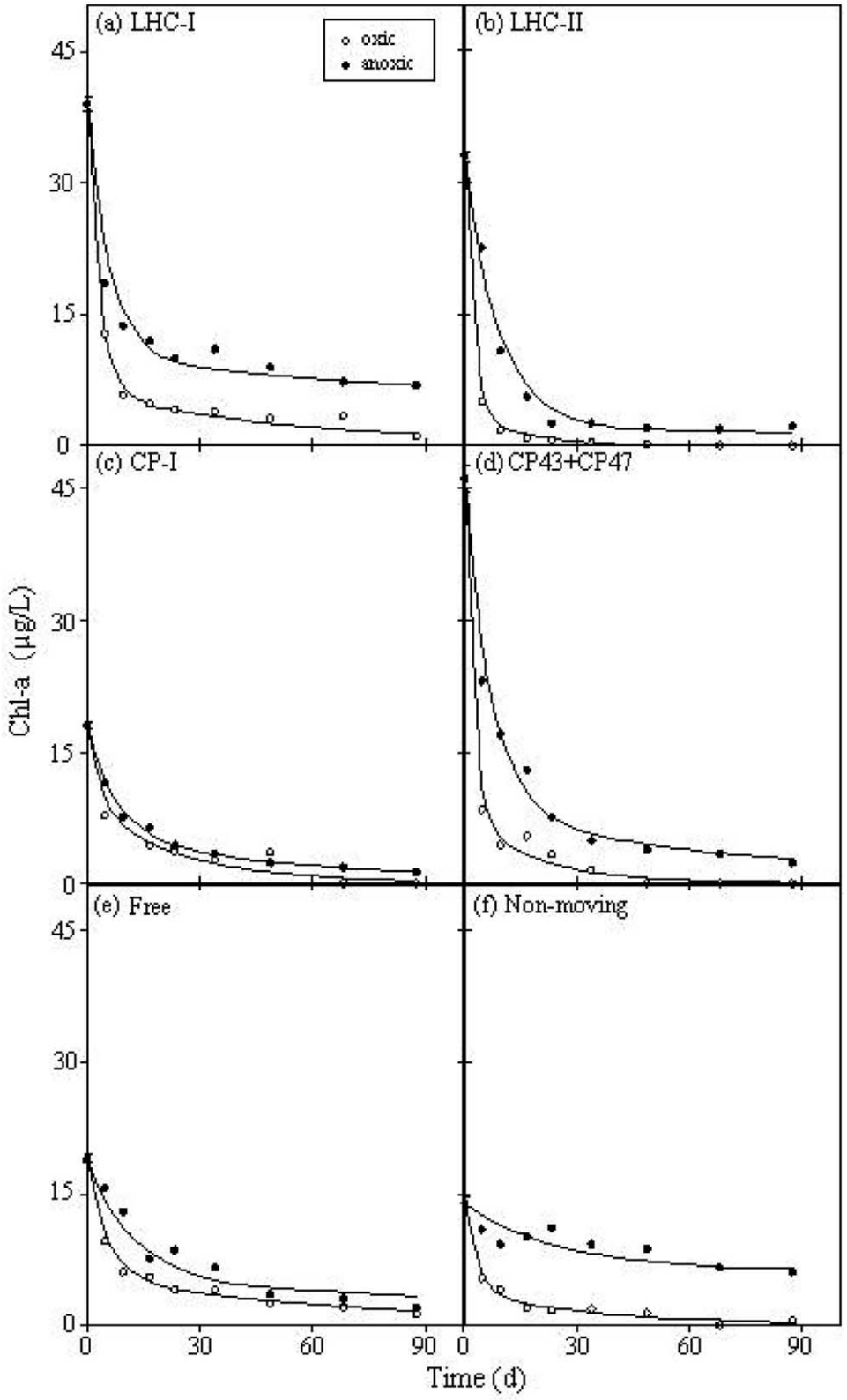


Fig. 6. Variations of Chl-a concentrations in various soluble structural component pools during incubations.

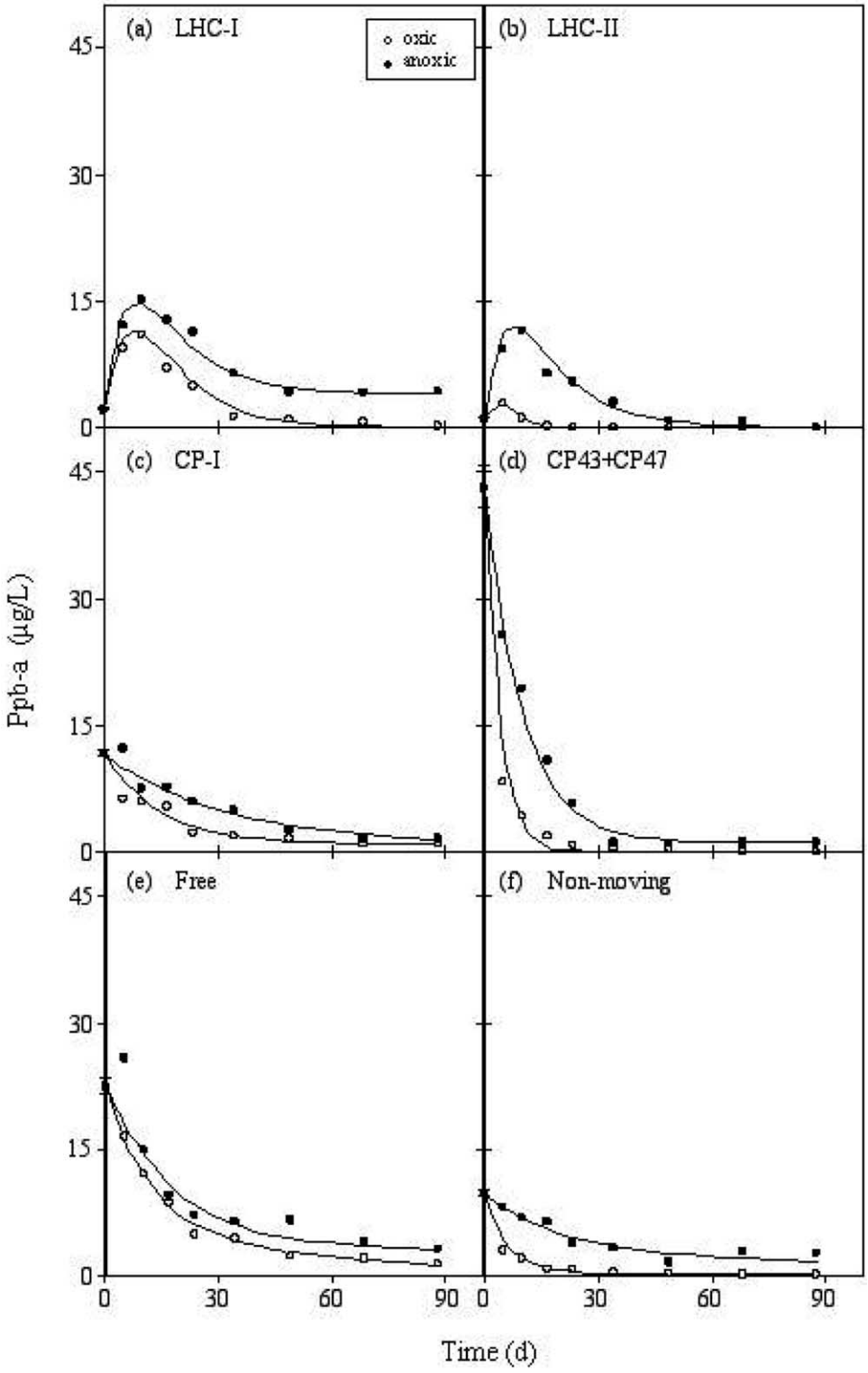


Fig. 7. Variations of Ppb-a concentrations in various soluble structural component pools during incubations.

the present study, intracellular Chl-a was bound in different structural components, as shown by our separation schemes (Fig. 1). Thus, Chl-a in these associations may have variable reactivities, resulting in different kinetic features during the degradation processes. Based on the G-model, we calculated the oxic and anoxic degradation rate constants of Chl-a in total pool, soluble and insoluble fractions, and all complex pools. However, the relative pool sizes varied substantially with frac-

Table 2. Degradation rate constants ($day^{-1}$) of Chl-a in total pigment pool (direct acetone extracted), different fractions and bands, and the ratios of rate constants between oxic and anoxic conditions.

| | Total Chl-a | Soluble fraction (F2) | Insoluble fraction (F3) | Non-moving (B1) | CP-1[a] (B2) | CP43 + CP47[b] (B3) | LHC-II[b] (B4) | LHC-I[a] (B5) | Free (B6) |
|---|---|---|---|---|---|---|---|---|---|
| $k_{ox1}$ | 0.27 | 0.328 | 0.055 | 0.261 | 0.248 | 0.415 | 0.445 | 0.302 | 0.173 |
| $k_{ox2}$ | 0.006 | 0.022 | 0 | 0.024 | 0.037 | 0.047 | 0.069 | 0.017 | 0.012 |
| $f_{ox1}$ (%) | 62.19 | 81.5 | 44.86 | 74.43 | 52.17 | 84.22 | 87.39 | 84.51 | 72.16 |
| $f_{ox2}$ (%) | 37.81 | 18.5 | 55.14 | 25.57 | 47.83 | 15.78 | 12.61 | 15.85 | 27.84 |
| $(k_{ox})_{av}$ | 0.17 | 0.271 | 0.025 | 0.200 | 0.147 | 0.357 | 0.398 | 0.258 | 0.128 |
| $k_{an1}$ | 0.08 | 0.115 | 0.012 | 0.041 | 0.124 | 0.137 | 0.109 | 0.145 | 0.081 |
| $k_{an2}$ | 0.004 | 0.009 | 0 | 0 | 0.015 | 0.012 | 0.004 | 0.004 | 0.005 |
| $f_{an1}$ (%) | 49.05 | 73.84 | 42.62 | 54.62 | 70.67 | 82.24 | 93.33 | 74.62 | 71.95 |
| $f_{an2}$ (%) | 50.95 | 26.16 | 57.38 | 45.36 | 29.33 | 17.76 | 6.67 | 25.38 | 28.05 |
| $(k_{an})_{av}$ | 0.042 | 0.087 | 0.005 | 0.022 | 0.092 | 0.115 | 0.102 | 0.109 | 0.06 |
| $k_{ox}/k_{an}$ | 4.05 | 3.11 | 5 | 9.09 | 1.6 | 3.1 | 3.9 | 2.37 | 2.13 |

[a] photosystem-I (PS-I);
[b] photosystem-II (PS-II).

tions and redox conditions. To compare the Chl-a degradation rate constants between oxic and anoxic conditions no matter how pool sizes varied, we used a new parameter, $k_{av}$, defined as the average degradation rate constant of two different pools:

$$k_{av} = k_1 \times f_1 + k_2 \times f_2 \quad (3)$$

where, $f_1$ and $f_2$ are relative proportions of pool 1 and pool 2 ($f_1 = (G_1)_0/(G_t)_0$ and $f_2 = (G_2)_0/(G_t)_0$). The pool sizes ($(G_1)_0$ and $(G_2)_0$) were estimated by plotting $\ln(G_t)$ vs. incubation time (t), which yields a breaking point to differentiate two pools. However, it is still unclear why the reactivity of Chl-a varies within a single structural fraction (e.g., protein or peptide complex).

Comparison of the Chl-a degradation rate constants (Table 2) showed several interesting implications. First, the $k_{ox}/k_{an}$ ratio of total Chl-a was ~4.0 but the ratios in various fractions and complexes ranged from ~2 to 9 (lower or higher than that of total Chl-a). This result implies that oxygen effects on Chl-a degradation are different among the various structural components. Second, Chl-a in the soluble fraction degraded much faster (> 10X) than that in insoluble fraction under both oxic and anoxic conditions. This suggests that physical and chemical properties of the major structural fractions control the reactivity of Chl-a bound in them. Third, the oxic degradation rate constants of Chl-a complexes in PS-II photosystem (LHC-II and CP43+CP47) were apparently (~2X) higher than those in PS-I photosystem (LHC-I and CP-I) while anoxic degradation rate constants of Chl-a complexes in two photosystems were almost the same. This indicates that two photosystems have different responses to oxic degradation processes but there are no different responses to anoxic degradation processes between them. Fourth, in the same photosystem, polypeptide complexes seemed to degrade somewhat faster than protein complexes under oxic conditions. This reflects that the binding features of polypeptides and proteins in these complexes affect Chl-a degradation in the complexes. And fifth, the oxic and anoxic degradation rate constants of Chl-a in free pigment pool were the smallest in almost all pools (except the case in anoxic non-moving pool). These rate constants may be underestimated because the decrease of free Chl-a concentration in the free pool is probably a net balance between release of Chl-a from other complex pools and its degradation within the free pool.

Previous studies have demonstrated that Chl-a is a labile organic compound with a turnover time ranging from 10 to 100 days in different environments (Leavitt and Carpenter, 1990; Bianchi and Findlay, 1991; Sun et al., 1993a, 1993b; Gerino et al., 1998; Bianchi et al., 2000). From this study, total cellular Chl-a turned over in ~6 days in oxic seawater and 24 days in anoxic seawater. These time scales are consistent with the estimation (44 turnovers per year) of global Chl-a degradation in the oceans (Whittaker, 1975). When intracellular Chl-a molecules were separated into different fractions, we could see that structural associations of Chl-a within the cells affected Chl-a reactivities and the responses to different redox conditions.

### 4.3. Relative Contributions of Various Pools to Total Chl-a Degradation

Degradation rate of Chl-a generally depends on the reactivity ($k$, degradation rate constant) and the pool size (G, concentration) when the first-order kinetics is followed (Sun et al., 1993a, 1993b; Ahmed et al., 2002; Josefson et al., 2002). As shown by the estimates from the multi-G model, the degradation rate constants of intracellular Chl-a varied with fractions and redox conditions (Table 2). To assess the relative contributions of each pool to the total degradation rate of Chl-a, we calculated the relative degradation rates of Chl-a in various fractions and complex pools by multiplying the degradation rate constants ($k$) with the relative pool sizes (concentration percentages relative to the total) (Table 3). In general, sum of relative degradation rates from two major fractions (soluble and insoluble) were close to the total degradation rates estimated from the total acetone extracted Chl-a. Although the relative size of insoluble fraction accounted for ~40% of the total Chl-a, the contributions to oxic and anoxic degradation rates of total Chl-a were very small (below 7%). The major cause for this low contribution is due to the high resistance of insoluble Chl-a to degradation processes. However, it is unclear what are structural configurations of insoluble Chl-a components within the cells and why they are refractory for oxic and anoxic degradations.

On the other hand, relative contributions of various Chl-a complexes to the oxic and anoxic degradation rates of soluble

Table 3. Relative degradation rate R′ (concentration %/day) and relative contribution (%) of the Chl-a degradation rate in each pool to the total Chl-a degradation rate.

| | Total Chl-a (T) | Soluble (F2) | Insoluble (F3) | Sum (F2 + F3) | Non-moving (B1) | CP-I (B2) | CP43 + CP47 (B3) | LHC-II (B4) | LHC-I (B5) | Free (B6) | Sum (B1–B6) |
|---|---|---|---|---|---|---|---|---|---|---|---|
| Chl-a % | 100 | 52.97 | 40.44 | 93.41 | 4.68 | 6.23 | 16.18 | 9.75 | 11.41 | 5.07 | 53.32 |
| $(k_{ox})_{av}$ | 0.17 | 0.271 | 0.025 | | 0.2 | 0.147 | 0.357 | 0.398 | 0.258 | 0.128 | |
| $R'_{ox}$ | 0.17 | 0.144 | 0.01 | 0.154 | 0.009 | 0.009 | 0.058 | 0.039 | 0.029 | 0.006 | 0.15 |
| (Rel. Cont. %) | | (93.5) | (6.49) | | (6.00) | (6.00) | (38.67) | (26.00) | (19.33) | (4.00) | |
| $(k_{an})_{av}$ | 0.042 | 0.087 | 0.005 | | 0.022 | 0.092 | 0.115 | 0.102 | 0.109 | 0.06 | |
| $R'_{an}$ | 0.042 | 0.046 | 0.002 | 0.048 | 0.001 | 0.006 | 0.019 | 0.01 | 0.014 | 0.003 | 0.053 |
| (Rel. Cont. %) | | (95.83) | (4.17) | | (1.89) | (11.32) | (35.85) | (18.87) | (26.41) | (5.66) | |

$R' = k_{av} \times$(Chl-a %).

Chl-a fraction varied from 2 to 39% (Table 3). The largest contributions (36%–39%) were from the CP43+CP47 complex pool in both oxic and anoxic systems. The reason for the largest contributions from the CP43+CP47 pool is because of larger pool size and higher reactivity. The contributions from LHC-I and LHC-II pools were moderate (from 18 to 26%). Under oxic conditions, the relative contribution from LHC-II was larger than that from LHC-I since the reactivity of Chl-a in LHC-II was ~1.5X larger than that in LHC-I although the relative pool size of LHC-II was somewhat smaller than that of LHC-I. In contrast, under anoxic conditions, the reactivities of Chl-a in both LHC-I and LHC-II were similar. Thus, the relative contributions from LHC-I and LHC-II depended more on the relative pool size, that is, greater contribution was from the LHC-I with a larger pool size. The other three pools, CP-I, non-moving, and free pigment each contributed less than 7% of total degradation in the oxic system but their contributions ranged from 2 to 11% in the anoxic system. The lower contributions of the three pools were presumably caused by smaller pool sizes. Sums of relative rate contributions from six soluble subpools were well equivalent to the rates from the soluble fraction in both oxic and anoxic systems. From these calculations, it is clear that the degradation of intracellular Chl-a was controlled by soluble components while the dominant contributions were from protein and polypeptide complexes (CP43+CP47, LHC-I and LHC-II).

### 4.4. Effects of Intracellular Structural Associations on Chl-a Degradation

Our experimental results showed that Chl-a complexes (CP43+CP47, and LHC-II) in PS-II had higher reactivities (larger $k$) than those (CP-I and LHC-I) in PS-I under oxic conditions. The difference in the reactivity of Chl-a complexes may be attributed to different structural configurations, functions and involved reactions between two photosystems. For example, PS-II performs a series of photochemical reactions to oxidize water during photosynthesis (Barber, 1998; Kraub, 2003) and a variety of toxic oxygen species such as singlet oxygen are generated simultaneously (Jung, 2004). To keep its stability and good performance, the PS-II system produces some antioxidants (e.g., carotenoids) and antioxidant enzymes (e.g., catalase and superoxide) or replaces damaged proteins with newly synthesized compounds (Brown, 1987; Barber, 1998; Tracewell et al., 2001; Jung, 2004). However, when the cells die, the PS-II stops producing antioxidants, antioxidant enzymes and new proteins. As a consequence, the PS-II is unable to protect their Chl-a complexes (LCH-II and CP43+CP47) from attack by oxygen species. Unlike PS-II, PS-I has a series of non-chlorophyll-bound proteins such as BtpA (a specific regulatory protein) and PS-I-F, I, J and K (small accessory protein or peptide subunits), which surround and stabilize the Chl-a complexes even after the death of the cells (Zak and Pakrasi, 2000; Scheller et al., 2001; Chitnis, 2001; Jensen et al., 2003). Therefore, protection of Chl-a complexes by other proteins in the PS-I may retard the degradation of Chl-a bound in this system. However, all Chl-a complexes in both PS-I and PS-II had similar reactivities under anoxic conditions although they were less reactive than those under oxic conditions. At the present, it remains unknown how anoxic processes affect degradation of Chl-a complexes although we observed a greater variation of bacterial abundance in the anoxic system.

Meanwhile, the differences in molecular size, structural binding mode, and location of various Chl-a complexes within the photsystems would be other factors affecting degradation behaviors. The protein complex CP-I in PS-I has a larger molecular size (160 kDa) than CP43+CP47 (~60 kDa) in PS-II while the LHC-I and LHC-II are small polypeptide complexes with molecular weights of 25–30 kDa (Barber et al., 1998, 2000; Fromme et al., 2001; Germano et al., 2002; Jackowski et al., 2003). The CP complexes, as core proteins, usually locate in the center of the photosytems and are surrounded by many other proteins and polypeptide complexes (Barber et al., 1998, 2002; Ben-Shem et al., 2003; Bibby et al., 2003; Jensen et al., 2003). On the other hand, the CP proteins and LHC polypeptides have different number of $\alpha$ helices, which play a critical role in protecting Chl-a in these complex structures (Barber et al., 2000; Fromme et al., 2001; Tetenkin, 2003; Ben-Shem et al., 2003). The largest Chl-a protein complex (CP-I) in the PS-I generally has 13 helices (Green and Durnford, 1996; Fromme et al., 2001). In the PS-II, two CP complexes (CP43 and CP47) have similar structures and each possesses 6 helices (Barber et al., 2000; Bumba and Vácha, 2003). The LHC-I and LHC-II polypeptide complexes in the PS-I and PS-II photosystems have 3 helices for each (Green and Durnfold, 1996; Croce et al., 2002; Germano et al., 2002). The combination of the large molecular size, a central location surrounded by other molecules, and more helices in CP-I com-

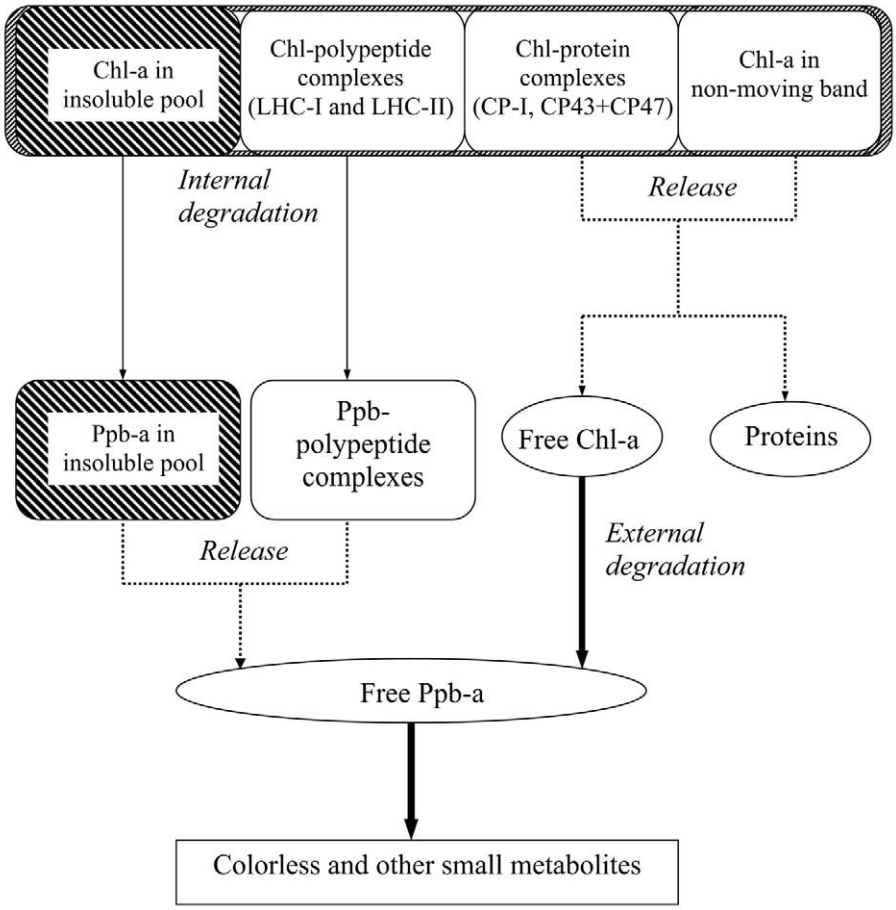


Fig. 8. Possible degradation pathways of chloropigments bound in various structural components of *E. hyxleyi* cells.

plex may provide an advantage in protecting the complex structure. By contrast, the Chl-a in LHC-I and LHC-II polypeptide complexes may be more readily degraded due to their small sizes, fewer helices, and edge locations in the photosytems.

### 4.5. Possible Degradation Pathways of Chl-a in Different Intracellular Structural Pools

Algal Chl-a can be degraded by various biologic and biochemical processes in nature (SooHoo and Kiefer, 1982; Welschmeyer and Lorenzen, 1985; Carpenter et al., 1986; Furlong and Carpenter, 1988; Louda et al., 1998). The primary degradation pathway of Chl-a involves production of several phaeopigments (Hendry et al., 1987). For example, Chl-a is converted to Ppt-a through loss of magnesium, to chlorophyllide-a through loss of phytol, and to Ppb-a through loss of both magnesium and phytol. In this study, we detected Ppb-a and Ppt-a as major phaeopigments in different intracellular fractions and complex pools, but the variations of Ppb-a were much greater and more closely related to Chl-a degradation than Ppt-a. Thus, we modeled the variations of Ppb-a in different pools to examine the possible degradation pathways of various Chl-a complexes.

During oxic and anoxic incubations, Ppb-a concentrations in different fractions and pools varied in two different patterns: (1) continuous decrease from the beginning of the incubations; and (2) initial increase in the first 10 days and followed by a continuous decrease over subsequent period. The first pattern was clearly observed in the CP complex pools and non-moving pool while the second pattern occurred in LHC complex pools and in insoluble fraction under both oxic and anoxic conditions. However, greater initial increases of Ppb-a concentration were always found in anoxic seawater, resulting in a Ppb-a concentration peak in the total pigment pool only in anoxic seawater (Fig. 4c). The initial build-up of Ppb-a concentration is likely caused by prevailing production of Ppb-a over degradation within some pools while continuous decrease of Ppb-a in other pools may be due to a lack of Ppb-a production.

Based on these results, we proposed a conceptual model to describe different degradation pathways of Chl-a in various structural pools (Fig. 8). The inverse correlation between initial Ppb-a increase and Chl-a decrease within the LHC pools and insoluble fraction indicates an internal degradation pathway, that is, Chl-a bound in these components might degrade inside the structural complexes and remain a link between Ppb-a and other molecular matrixes. In contrast, Chl-a molecules bound in

Table 4. Release and degradation rate constants ($day^{-1}$) of Ppb-a in various soluble structural component pools.

| | Release | | | Degradation | | |
|---|---|---|---|---|---|---|
| | $(k_r)_{ox}$ | $(k_r)_{an}$ | $(k_r)_{ox}/(k_r)_{an}$ | $(k_d)_{ox}$ | $(k_d)_{an}$ | $(k_d)_{ox}/(k_d)_{an}$ |
| LHC-I | 0.122 | 0.169 | 0.72 | 0.101 | 0.079 | 1.28 |
| LHC-II | 0.325 | 0.18 | 1.81 | 0.31 | 0.081 | 3.83 |
| CP-I | na | na | na | 0.067 | 0.035 | 1.92 |
| CP43 + CP47 | na | na | na | 0.245 | 0.099 | 2.48 |
| Free | na | na | na | 0.094 | 0.047 | 2.00 |
| Non-moving | na | na | na | 0.168 | 0.036 | 4.67 |

na: not availabl

the CP complexes and in the non-moving pool have to be released from the structural complexes into free pigment pool before they degrade into Ppb-a. In addition, the Ppb-a bound in LHC complexes need to be released into free pigment pool before further degradation into colorless or other small metabolites. Due to high labilities of free Chl-a and Ppb-a, both compounds cannot significantly accumulate in the free pool.

Sun et al. (1993a) applied a kinetic model to quantify release and degradation rates of bound and free Chl-a in sediments. In this study, we adopted this model to quantify the release and degradation rates of Ppb-a in various structural pools. Total Ppb-a concentration ($C_t$) is first separated into the released Ppb-a ($C_a$), which is from internal degradation of Chl-a, and the free Ppb-a ($C_f$). Within the free pool, there are two Ppb-a fractions: fast degradable $C_{f1}$ and slow or non-degradable $C_{f2}$. The time-dependent variation of $C_t$ (degradation rate) can be expressed as:

$$\frac{dC_t}{dt} = \frac{dC_a}{dt} + \frac{dC_f}{dt} = k_r C_a - k_{d1} C_{f1} - k_{d2} C_{f2} \qquad (4)$$

where $k_r$ is the first-order release rate constant of Ppb-a from internal Chl-a degradation; $k_{d1}$ and $k_{d2}$ are the first-order degradation rate constants of $C_{f1}$ and $C_{f2}$. Since the $k_{d2}$ is very small (close to 0) in most cases, the solution of eqn. (4) becomes:

$$C_r = \frac{k_r (C_a)_0}{k_{d1} - k_r} [\exp(-k_r t) - \exp(-k_{d1} t)] + (C_{f1})\exp(-k_{d1} t) + (C_{f2})_0 \qquad (5)$$

We assume that at $t = 0$, $(C_t) = (C_f)_0 = (C_{f1})_0 + (C_{f2})_0$; as $t \to \infty$, $(C_t) = (C_{f2})_t$; and $(C_a)_0$ is the potential concentration of Ppb-a if Chl-a in each pool is degraded to Ppb-a. Fitting the Ppb-a data from LHC pools to eqn (5), the rate constants $k_r$ and $k_d$ (that is $k_{d1}$ when $k_{d2} = 0$) can be estimated (Table 4). For the cases of continuous decrease in Ppb-a concentration during incubation, the degradation rate constants (Table 4) were estimated based on the eqn. (2).

Comparison of Ppb-a release and degradation rate constants between two polypeptide complexes (LHC-I and LHC-II) showed that a large difference (~3X) occurred only in oxic seawater and the rate constants were similar in anoxic seawater, which was consistent with the cases of Chl-a degradation. For protein complexes (CP-I and CP43+CP47), larger degradation rate constants (oxic and anoxic) occurred in PS-II than in PS-I. These results imply that the superstructures of photosystems may affect the production and degradation of Ppb-a, as they do for Chl-a. Moreover, chloropigments in PS-II may have a more sensitive response to oxic conditions than those in PS-I although they have similar behaviors under anoxic conditions.

## 5. CONCLUSIONS

Detailed examination of chloropigment degradation in natural oxic and anoxic seawaters reveals that the intracellular structural associations of pigments with various molecular matrixes have important influences on Chl-a degradation. Soluble protein and polypeptide complexes of Chl-a are major pools of reactive pigments, which contribute ~90% of overall degradation. Chl-a in the PS-II degraded generally faster than that in the PS-I, especially under oxic conditions, implying that the sizes, constitutions, and functions of these superstructural photosystems may control the fate of individual pigment compounds during biochemical degradation processes. The structural features of various complexes also control the degradation pathways of Chl-a, leading to internal degradation of Chl-a to Ppb-a within the complex pools or external degradation after release from the complexes. In summary, the intracellular structural associations among organic compounds may be an important factor affecting degradation/preservation of organic matter in natural environments.

*Acknowledgments*—We wish to thank M. I. Scranton and her group for help with collecting oxic and anoxic seawaters from the Cariaco Basin. This research was supported by NSF grant OCE-0116786 and ACS grant 35068-AC.

*Associate editor:* C. Arnosti

## REFERENCES

Ahmed J. A., Kaur A. and Shivhare U. (2002) Color degradation kinetics of spinach, mustard leaves and mixed puree. *J. Food Sci.* **67,** 1088–1091.

Almela L., Fernández-López J. A. and Roca M. J. (2000) High-performance liquid chromatographic screening of chlorophyll derivatives produced during fruit storage. *J. Chromatogr. A* **870,** 483–489.

Barber J. (1998) Photosystem two. *BBA-Bioenerg.* **1365,** 269–277.

Barber J., Morris E. and Büchl C. (2000) Revealing the structure of the photosystem II chlorophyll binding proteins, CP43 and CP47. *BBA-Bioenerg.* **1459,** 239–247.

Barber J. (2002) Photosystem II: a multisubunit membrane protein that oxidizes water. *Cur. Opi. Struct. Bio.* **12,** 523–530.

Barrett J. and Jeffrey S. W. (1971) A note on the occurrence of chlorophyllase in marine algae. *J. Exp. Mar. Biol. Ecol.* **7,** 255–262.

Ben-Shem A., Frolow F. and Nelson N. (2003) Crystal structure of plant photosystem I. *Nature* **426,** 630–635.

Berger W. H. and Keir R. S. (1984) Glacial-Holocene changes in atmospheric $CO_2$ and the deep-sea record. In *Climate Processes and Climate Sensitivity* (eds. J. E. Hansen and T. Takahashi) pp. 337–351, AGU, Washington, DC.

Berner R. A. (1980) Early Diagenesis: A Theoretical Approach. Princeton University Press, Princeton, N. J.

Bianchi T. S. and Findlay S. (1991) Decomposition of Hudson estuary marcrophytes-Photosynthetic pigment transformation and decay constants. *Estuar.* **14,** 65–73.

Bianchi T. S., Johansson B. and Elmgren R. (2000) Breakdown of phytoplankton pigments in Baltic sediments: effects of anoxia and loss of deposit-feeding macrofauna. *J. Exp. Mar. Bio.* **251,** 161–183.

Bibby T. S., Nield J., Chen M., Larkum A. W. D. and Barber J. (2003) Structure of a photosystem II supercomplex isolated from *Prochloron didemni* retaining its chlorophyll a/b light-harvesting system. *PNAS* **100,** 9050–9054.

Brown J. (1987) Functional organization of chlorophyll-a and carotenoids in the alga, *Nannochloropsis salina*. *Plant Physiol.* **83,** 434–437.

Bumba L. and Vácha F. (2003) Electron microscopy in structural studies of Photosystem II. *Photosys. Res.* **77,** 1–19.

Carpenter S. R., Elser M. and Elser J. J. (1986) Chlorophyll production, degradation and sedimentation: Implication for paleolimnoloty. *Limnol. Oceanogr.* **31,** 112–124.

Chen N., Bianchi T. S. and Bland J. M. (2003) Novel decomposition products of chlorophyll-a in continental shelf (LA Shelf) sediments: formation and transformation of carotenol chlorin esters. *Geochim. Cosmochim. Acta* **67,** 2027–2042.

Chitnis R. R. (2001) Photosystem I: function and physiology. *Ann. Rev. Plant Physiol. Plant Mol. Bio.* **52,** 593–626.

Cranwell P. A., Eglinton G. and Robinson N. (1987) Lipids of aquatic organisms as potential contributors to lacustrine sediments—II. *Org. Geochem.* **11,** 513–527.

Croce R., Morosinotto T., Castelletti S., Breton J. and Bassi R. (2002) The Lhca antenna complexes of higher plants photosystem I. *BBA-Bioenerg.* **1556,** 29–40.

Danovaro R., Fabiano M. and Boyer M. (1994) Seasonal changes of benthic bacteria in a seagrass bed (*Posidonia oceanica*) of the Ligurian Sea in relation to origin, composition and fate of the sediment organic matter. *Mar. Biol.* **119,** 489–500.

Ding H. and Sun M.-Y. (2005) Biochemical degradation of algal fatty acids in oxic and anoxic sediment-seawater interface systems: effects of structural association and relative roles of aerobic and anaerobic bacteria. *Mar. Chem.* **93,** 1–19.

Fromme P., Jordan P. and Kraub N. (2001) Structure of photosystem I. *BBA-Bioenerg.* **1507,** 5–31.

Furlong E. T. and Carpenter R. (1988) Pigment preservation and remineralization in oxic coastal marine sediments. *Geochim. Cosmochim. Acta* **52,** 87–99.

Gerino M., Aller R. C., Lee C., Cochran J. K., Aller J. Y., Green M. A. and Hirschberg D. G. (1998) Comparison of different tracers and methods used to quantify bioturbation during a spring bloom: 234-thorium, luminophores and chlorophyll-a. *Est. Coast. Shelf Sci.* **46,** 531–547.

Germano M., Yakushevska A. E., Keegstra W., van Gorkom H. J., Dekker J. P. and Boekema E. J. (2002) Supramolecular organization of photosystem I and light-harvesting complex I in *Chlamydomonas reinhardtii*. *FEBS Lett.* **525,** 121–125.

Golbeck J. H. (1992) Structure and function of photosystem I. *Ann. Rev. Plant Physiol. Plant Mol. Biol.* **43,** 293–324.

Green B. R. and Durnford D. G. (1996) The chlorophyll-carotenoid proteins of oxygenic photosynthesis. *Ann. Rev. Plant Physiol. Plant Mol. Biol.* **47,** 685–714.

Harvey H. R., Tuttle J. H. and Bell J. T. (1995) Kinetics of phytoplankton decay during simulated sedimentation: Changes in biochemical composition and microbial activity under oxic and anoxic conditions. *Geochim. Comochim. Acta* **59,** 3367–3377.

Harvey H. R. and Macko S. A. (1997) Kinetics of phytoplankton decay during simulated sedimentation: Changes in lipids under oxic and anoxic conditions. *Org. Geochem.* **27,** 129–140.

Hendry G. A. F., Houghton J. D. and Brown S. B. (1987) The degradation of chlorophyll—a biological enigma. *New Phytol.* **107,** 205–302.

Henrichs S. M. and Doyle A. P. (1986) Decomposition of $^{14}C$-labeled organic-substance in marine sediments. *Liminol. Oceanogr.* **31,** 765–778.

Ikeda T. and Tajika E. (2003) Carbon cycling and climate change during the last glacial cycle inferred from the isotope records using an ocean biogeochemical carbon cycle model. *Global Planet Change* **35,** 131–141.

Itagaki T., Nakayama K. and Okada M. (1986) Chlorophyll-protein complexes associated with photosystem I isolated from the green alga, *Bryopsis maxima*. *Plant Cell Physiol.* **27,** 1241–1247.

Jackowski G., Olkiewicz P. and Zelisko A. (2003) The acclimative response of the main light-harvesting chlorophyll a/b-protein complex of phososystem II (LHC-II) to elevated irradiances at the level of trimeric subunits. *J. Photochem. Photobio. B-Bio.* **70,** 163–170.

Jensen P. E., Haldrup A., Rosgaard L. and Scheller H. V. (2003) Molecular dissection of photosystem I in higher plants: topology, structure and function. *Physiol. Plant.* **119,** 313–321.

Josefson A. B., Forbes T. L. and Rosenberg R. (2002) Fate of phytodetritus in marine sediments: functional importance of macrofaunal community. *Mar. Ecol-Prog. Ser.* **230,** 71–85.

Jung S. (2004) Variation in antioxidant metabolism of young and mature leaves of *Arabidopsis thaliana* subjected to drought. *Plant Sci.* **166,** 459–466.

Kashino Y. (2003) Separation methods in the analysis of protein membrane complexes. *J. Chromatogr. B* **797,** 191–216.

Keely B. J. and Brereton R. G. (1985) Early chlorin diagenesis in a recent aquatic sediment. *Org. Geochem.* **10,** 975–980.

Keely B. J. and Maxwell J. R. (1991) Structural characterization of the major chlorins in a Recent sediment. *Org. Geochem.* **17,** 663–669.

Keith-Roach M. J., Bryan N. D., Bardgett R. D. and Livens F. R. (2002) Seasonal changes in the microbial community of a salt marsh, measured by phospholipids fatty acid analysis. *Biogeochem.* **60,** 77–96.

King L. L. and Repeta D. J. (1994) High molecular-weight and acid extractable chlorophyll degradation products in the Black sea: new sinks for chlorophyll. *Org. Geochem.* **21,** 1243–1255.

Kraub N. (2003) Mechanisms for photosystems I and II. *Curr. Opinion Chem. Bio.* **7,** 540–550.

Leavitt P. R. and Carpenter S. R. (1990) Aphotic pigment degradation in the hypolimnion—implications for sedimentation studies and paleolimnology. *Limnol. Oceanogr.* **35,** 520–534.

Liu Z., Yan H., Wang K., Kuang T., Zhang J., Gui L., An X. and Chang W. (2004) Crystal structure of spinach major light-harvesting complexes at 2.72 Å resolution. *Nature* **428,** 287–292.

Louda J. W., Liu J., Liu L., Winfree M. N. and Baker E. W. (1998) Chlorophyll-a degradation during cellular senescence and death. *Org. Geochem.* **29,** 1233–1251.

Madrid V. M., Taylor G. T., Scranton M. I. and Chistoserov A. Y. (2001) Phylogenetic diversity of bacterial and archaeal communities in the anoxic zone of the Cariaco Basin. *Appl. Environ. Microbiol.* **67,** 1663–1674.

Mantoura R. F. C. and Llewellyn C. A. (1983) The rapid determination of algal chlorophyll and carotenoid pigments and their breakdown products in natural waters by reverse-phase high-performance liquid chromatography. *Anal. Chim. Acta* **151,** 297–314.

Neretin L. N., Bottcher M. E. and Grinenko V. A. (2003) Sulfur isotope geochemistry of the Black Sea water column. *Chem. Geol.* **200,** 59–69.

Ocampo R. and Repeta D. J. (1999) Structural determination of purpurin-18 (as methyl ester) from sedimentary organic matter. *Org. Geochem.* **30,** 189–193.

Ocampo R., Sachs J. P. and Repeta D. J. (1999) Isolation and structure determination of the unstable 13(2), 17(3)-cyclopheophorbide a enol from recent sediments. *Geochim. Cosmochim. Acta* **63,** 3743–3749.

Parkes R. J. and Taylor J. (1983) The relationship between fatty acid distributions and bacterial respiratory types in contemporary marine sediments. *Est. Coast. Shelf Sci.* **16,** 173–189.

Pedersen T. F. and Calvert S. E. (1990) Anoxia vs. productivity—What controls the formation of organic-carbon-rich sediment and sedimentary-rocks. *AAPG Bull.* **74,** 454–466.

Picaud A., Acker S. and Duration J. (1982) A single step separation of PS 1, PS 2 and chlorophyll-antenna particles from spinach chloroplasts. *Photosys. Res.* **3,** 203–313.

Porter K. G. and Feig Y. S. (1980) The use of DAPI for identifying and counting aquatic microflora. *Limnol. Oceanogr.* **25,** 943–948.

Puddu A., La Ferla R., Allegra A., Baddi C., Lopez M., Oliva F. and Pierotti C. (1998) Seasonal and spatial distribution of bacterial production and biomass along a salinity gradient (Northern Adriatic Sea). *Hydrobiol.* **363,** 271–282.

Saliot A., Derieux S., Sadouni N., Bouloubassi I., Fillaux J., Dagaut J., Momzikoff A., Gondry G., Builou C., Breas O., Gauwet G. and Deliat G. (2002) Winter and spring characterization of particulate and dissolved organic matter in the Danube-Black Sea mixing zone. *Est. Coast. Shelf Sci.* **54,** 355–367.

Schaeffer O., Ocampo R., Callot H. J. and Albrech P. (1993) Extraction of bound porphyrins from sulphur-rich sediments and their use for reconstruction of paleoenvironments. *Nature* **364,** 133–136.

Scheller H. V., Jensen P. E., Haldrup A., Lunde C. and Knoetzel J. (2001) Role of subunits in eukaryotic photosystem I. *Biochim. Biophys. Acta* **1507,** 41–60.

Schoch S. and Brown J. (1987) The action of chlorophyllase on chlorophyll-protein complexes. *J. Plant Physiol.* **126,** 483–494.

Soohoo J. B. and Kiefer D. A. (1982) Vertical-distribution of phaeopigments. 2. Rates of production and kinetics of photo-oxidation *Deep-Sea Res.* **19,** 1553–1563.

Squier A. H., Hodgson D. A. and Keely B. J. (2002) Sedimentary pigments as markers for environmental change in an Antarctic lake. *Org. Geochem.* **33,** 1655–1665.

Sun M.-Y., Aller R. C. and Lee C. (1991) Early diagenesis of chlorophyll-a in Long Island Sound sediments: A measure of carbon flux and particle reworking. *J. Mar. Res.* **49,** 379–401.

Sun M.-Y., Lee C. and Aller R. C. (1993a) Laboratory studies of oxic and anoxic degradation of chlorophyll-a in Long Island Sound sediment. *Geochim. Cosmochim. Acta* **57,** 147–157.

Sun M.-Y., Lee C. and Aller R. C. (1993b) Anoxic and oxic degradation of $^{14}$C-labeled chloropigments and a $^{14}$C-labeled diatom in Long Island Sound sediments. *Limnol. Oceanogr.* **38,** 1438–1451.

Sun M.-Y. and Wakeham S. G. (1998) A study of oxic/anoxic effects on degradation of sterols at the simulated sediment-water interface of coastal sediment. *Org. Geochem.* **28,** 773–784.

Sun M.-Y., Zou L., Dai J., Ding H., Culp R. A. and Scranton M. I. (2004) Molecular carbon isotopic fractionation of algal lipids during decomposition in natural oxic and anoxic seawaters. *Org. Geochem.* **35,** 895–908.

Suzuki M. T., Sherr E. B. and Sherr B. F. (1993) DAPI direct counting underestimates bacterial abundance and average cell-size compared to AO direct counting. *Limnol. Oceanogr.* **38,** 1566–1570.

Taylor G. T., Iabichella M., Ho T.-Y., Scranton M. I., Thunell R. C., Muller-Karger F. E. and Varela R. (2001) Chemoautotrophy in the redox transition zone of the Cariaco Basin: a significant midwater source of organic carbon production. *Limnol. Oceanogr.* **46,** 146–163.

Teece M. A., Getliff J. M., Leftley J. W., Parker R. J. and Maxewell I. R. (1998) Microbial degradation of the marine prymnesiophyte *Emiliania huxleyi* under oxic and anoxic conditions as a model for early diagenesis: long chain alkadienes, alkenones and alkyl alkenoates. *Org. Geochem.* **29,** 863–880.

Tetenkin V. L. (2003) Structural-functional organization of the main light harvesting complexes and photosystem 2 of higher plants. *Biochem. (Moscow)* **68,** 810–827.

Tracewell C. A., Vrettos J. S., Bautista J. A., Frank H. A. and Brudvig G. W. (2001) Carotenoid photooxidation in photosystem II. *Arch. Biochem. Biophy.* **385,** 61–69.

Tuttle J. H. and Jannasch H. W. (1977) Microbial dark assimilation of $CO_2$ in the Cariaco Trench. *Limnol. Oceanogr.* **24,** 746–753.

Vetriani C., Tran H. V. and Kerkhof L. J. (2003) Fingerprinting microbial assemblages from the oxic/anoxic chemocline of the Black Sea. *Appl. Environ. Microbiol.* **69,** 6481–6488.

Wakeham S. G. and Ertel J. R. (1987) Diagenesis of organic matter in suspended particles and sediments in the Cariaco Trench. *Org. Geochem.* **13,** 815–822.

Wakeham S. G. and Berier J. A. (1991) Fatty acid and sterol biomarkers as indicators of particulate matter source and alteration processes in the Black Sea. *Deep-Sea Res.* **38 Suppl. 2),** S943–S968.

Wakeham S. G. (1995) Lipid biomarkers for heterotrophic alteration of suspended particulate organic matter in oxygenated and anoxic water column of the ocean. *Deep-Sea Res. Part I* **42,** 1749–1771.

Wakeham S. G., Hopmans E. C., Schouten S. and Damsté J. S. S. (2004) Archaeal lipids and anaerobic oxidation of methane in euxinic water columns: a comparative study of the Black Sea and Cariaco Basin. *Chem. Geol.* **205,** 427–442.

Welschmeyer N. A. and Lorenzen C. L. (1985) Chlorophyll budgets: Zooplankton grazing and phytoplankton growth in a temperate fjord and the Central Pacific Gyre. *Limnol. Oceanogr.* **30,** 1–21.

Westrich J. T. and Berner R. A. (1984) The role of sedimentary organic matter in bacterial sulfate reduction: The G model tested. *Limnol. Oceanogr.* **29,** 236–249.

Whittaker R. H. (1975) Communities and Ecosystems (2nd Edn.). Macmillan, New York.

Zak E. and Pakrasi H. B. (2000) The BtpA protein stabilizes the reaction center proteins of photosystem I in the cyanobacterium *Sumechocystis* sp. PCC 6803 at low temperature. *Plant Physio.* **123,** 215–222.

Zolla L., Biancheti M., Timperio A. M. and Corradini D. (1997) Rapid resolution by reversed-phase high-performance liquid chromatography of the thylakoid membrane proteins of the photosystem II light-harvesting complex. *J. Chromatogr. A* **779,** 131–138.

Zweifel U. L., Blackbum N. and Hagström A. (1996) Cycling of marine dissolved organic matter. I. An experimental system *Aquat. Microb. Ecol.* **11,** 65–77.